

OPEN

The N-terminal Acetylation of α -Synuclein Changes the Affinity for Lipid Membranes but not the Structural Properties of the Bound State

Matteo Runfola¹, Alfonso De Simone¹, Michele Vendruscolo^{1,2}, Christopher M. Dobson^{1,2,3} & Giuliana Fusco^{2*}

The aggregation of α -synuclein (α S), a protein abundant at presynaptic terminals, is associated with a range of highly debilitating neurodegenerative conditions, including Parkinson's disease (PD), dementia with Lewy bodies (DLB) and multiple system atrophy (MSA). Emerging evidence indicates that the interaction of α S with lipid membranes defines both its physiological function and pathological effects. The characterisation of the modes of membrane binding by α S is therefore crucial to clarify the balance between normal and aberrant behaviour of this protein. Here we used solid-state nuclear magnetic resonance (ssNMR) spectroscopy to probe the nature of the N-terminally acetylated form of α S (NTAc- α S) bound to synaptic-like lipid vesicles. This post-translational modification is prevalent for the physiological form of α S and modulates the binding to lipid bilayers. By probing the structure, dynamics and membrane topology of NTAc- α S, we found that N-terminal acetylation does not alter significantly the conformational and topological properties of the membrane-bound state of α S, despite increasing its propensity for binding. Taken together, our data and previous characterisations of the cytosolic state of NTAc- α S clarify that the role of the N-terminal acetylation is to regulate the binding affinity of α S for synaptic vesicles without altering the structural properties of the bound state.

α -Synuclein (α S) is a 14 kDa monomeric disordered protein preferentially found at pre-synaptic termini¹. The aggregation of α S is strongly linked with Parkinson's disease (PD)^{2–6}, as its aggregates are the major constituents of Lewy bodies in PD patients^{7–9}. Point mutations, as well as duplications and triplications, in the α S gene are also associated with familial forms of PD^{10–15}, and fibrillar aggregates of the non-amyloid- β component (NAC) region of the protein (residues 61–95) are associated with Alzheimer's disease¹⁶.

The function of α S is currently still debated. Several lines of evidence have indicated a possible role for this protein in the regulation of the trafficking of synaptic vesicles (SVs)¹⁷, including the maintenance of pools of SVs at the synaptic termini^{18–22}, the promotion of interactions between SVs^{23–26} and the assistance of SNARE formation during neurotransmitter release^{27–30}. α S has also been shown to bind mitochondrial membranes, where it may have role in the mitigation of oxidative stress of mitochondria^{31–33}. A common characteristic of the majority of these putative functions is that they all require the binding of α S to lipid membranes³⁴. Indeed, the partition between membrane-bound and cytosolic forms of α S is tightly regulated *in vivo*³⁵ and appears to be crucial for the mechanism of α S aggregation^{21,36–41} as well as the toxicity of its fibrillar oligomers⁴². Understanding the biological regulation of this interaction is therefore a major priority to clarify the balance between functional and dysfunctional aspects in this presynaptic protein.

Upon membrane binding α S undergoes a transition from an intrinsically disordered monomeric protein^{43–45} to a conformation that is enriched in α -helical structure. This ordering process is promoted by 7 imperfect sequence repeats of 11 residues located in the first 90 residues of the protein sequence and encoding for amphipathic α -helical motifs⁴⁵. The modular organization of the repeats provides α S with the ability to bind a variety

¹Department of Life Sciences, Imperial College London, SW7 2AZ, London, UK. ²Department of Chemistry, University of Cambridge, Cambridge, CB2 1EW, UK. ³Christopher M. Dobson is deceased. *email: gf203@cam.ac.uk

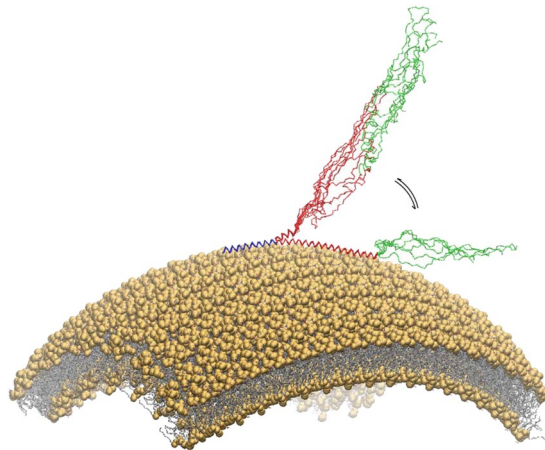


Figure 1. Representation of the SUV-bound state of α S. Schematic illustration of the binding mode of α S to a lipid vesicle. Three regions of protein have different dynamical and structural properties upon binding with the membrane⁴⁴. The 25 N-terminal residues (blue) are rigidly anchored to the membrane surface, adopting a stable α -helical conformation. The central region, spanning residue 26–98 (red), is in equilibrium between bound-tethered and unbound-detached conformations. The C-terminal region (residues 98–140, green) remains unstructured and weakly associated with the membrane surface.

of assemblies ranging from small detergent micelles to lipid vesicles and membranes^{43,46,47} using a multiplicity of distinct binding modes⁴³.

Membrane binding by α S is modulated by some post-translational modifications (PTMs), including the phosphorylation of different residues in the sequence^{48–50}. Moreover, the N-terminal acetylation of α S^{51,52}, which is found in both healthy individuals and PD patients, has been shown to induce stronger membrane affinity, as well as an increased propensity to adopt transient α -helical structures in the N-terminal region^{53,54}, a property that is enhanced upon copper interaction^{55,56}.

As the N-terminally acetylated α S (NTAc- α S) is considered to be the physiologically relevant form, and because of the central role of membrane binding for both functional and pathological contexts, it is important to investigate how this PTM alters the structure and dynamics of the membrane bound state of α S. Although previous studies have analysed the interaction between NTAc- α S and lipid membranes by probing the properties of its unbound state^{50,53,54,57}, a full understanding of the structural and dynamical properties of the membrane-bound state of NTAc- α S is currently missing.

To answer to this key question, we here employed solid-state NMR (ssNMR) to directly probe the conformational properties of NTAc- α S at the surface of small unilamellar vesicles (SUVs) that mimic synaptic vesicles for composition and size^{43,44}. Using an approach based on paramagnetic relaxation enhancement (PRE) effects, we investigated the impact of the N-terminal acetylation on the topological properties of the protein with respect to the lipid membrane. Our experiments elucidated the nature of the membrane-bound state of NTAc- α S and clarified further the role of this PTM on the regulation of the membrane interaction of α S.

Results

ssNMR spectra of NTAc- α S bound to lipid vesicles. Previous magic angle spinning (MAS) ssNMR studies of non-acetylated α S identified three different regions of the protein having distinctive structural and dynamical properties in the membrane-bound state⁴⁴. These regions include the N-terminal portion of the protein, which spans the initial 25 residues and acts as the primary membrane-binding motif that adopts the conformation of a stable amphipathic helix anchoring the protein onto the membrane surface. It was possible to assign the ssNMR resonances of the segment 6–25 of this region⁴⁴ and employ these data to refine its structural ensemble when bound to synaptic-like vesicles⁵⁸. In addition to the rigid N-terminal anchor, a central ‘sensor’ region (residues 26 to 98) resulted to have enhanced relaxation properties in the ssNMR spectra, suggesting that it exists in equilibrium between multiple conformations at the membrane surface (Fig. 1)⁴⁴. The central region was shown to modulate the overall affinity of the protein for lipid bilayers⁴⁴ as well as to be involved in the mechanism by which α S promotes the clustering of synaptic vesicles²³. Finally, the C-terminal residues (99 to 140) were found to remain largely unstructured and unbound to lipid bilayers, with some residues establishing transient contacts with the membrane surface⁴⁴.

We here used ssNMR to investigate the effects of N-terminal acetylation to the membrane-bound form of α S. ¹³C-¹⁵N labelled NTAc- α S samples were mixed with DOPE:DOPS:DOPC (5:3:2 w/w) SUVs at a protein:lipid ratio of 1:65⁴⁴ and pelleted via ultracentrifugation into 3.2 mm rotors for MAS ssNMR. ¹³C-¹³C dipolar assisted rotational resonance (DARR)⁵⁹ spectra of membrane-bound NTAc- α S, which were measured at -19°C to enhance the signal to noise under conditions where this lipid mixture adopts a gel phase⁶⁰, revealed a number of resonances belonging to residues from the N-terminal region in a rigid bound state at the surface of the SUVs (Fig. 2a). A close inspection of the resonances from these spectra revealed no significant differences between the chemical shifts of the membrane bound states of NTAc- α S and non-acetylated α S⁴⁴. Similarly, by analysing the

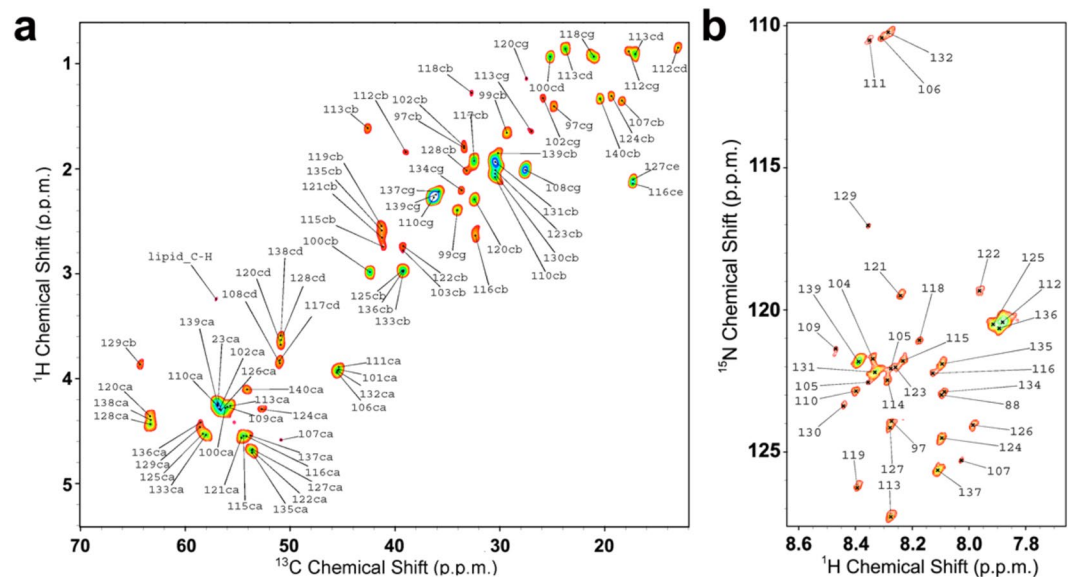


Figure 3. INEPT-based identification of dynamical regions of NTAc- α S bound to DOPE:DOPS:DOPC SUVs. ^{13}C -detected ^1H - ^{13}C correlation via INEPT transfer (a) and ^1H -detected ^1H - ^{15}N -HSQC (b) of NTAc- α S bound to DOPE:DOPS:DOPC SUVs recorded at 4°C using MAS ssNMR with spinning rate of 10 kHz. The experiments were performed at a ^1H Larmor frequency of 700 MHz using a 3.2 mm E^{Free} probe. Atom names ca, cb, cg, cd are used for C^α , C^β , C^γ and C^δ atoms, respectively. Assignment of the spectra were derived from previous studies of vesicle bound α S⁴⁴.

residues spanning the region 97 to 140 of the protein, and showed no considerable differences with the chemical shifts measured using both monomeric-disordered α S in water and non-acetylated α S at the surface of SUVs.

Taken together, ssNMR experiments indicated that the dynamical and structural properties of both rigid and disordered regions of α S bound to the surface of lipid bilayers do not change significantly as a result of the N-terminal acetylation.

Membrane insertion of the N-terminal anchor of NTAc- α S. Next, we used ssNMR to directly probe the topological properties of the membrane-bound state of NTAc- α S. In particular, using paramagnetic relaxation enhancement (PRE)^{64,65} experiments, we could obtain detailed information of the levels of protein insertion into the hydrophobic region of the lipid bilayer. These experiments were performed by doping the DOPE:DOPS:DOPC lipid mixture with low quantities (2%) of lipids that incorporate a paramagnetic centre into their chemical structure. The spatial vicinity of protein regions to this centre enhances the transverse relaxation of their NMR signals, thereby providing a map of the contacts between the protein and the spin. Four different types of paramagnetic lipids were used to obtain a map of the contacts between the protein and spins placed at different positions of the membrane, i.e. from the hydrophilic head groups to the last carbon of the hydrophobic tail (Fig. 4). PRE measured via ^{13}C - ^{13}C -DARR spectra by doping the membrane with a paramagnetic centre in head groups (gadolinium salt of PE-DTPA, Avanti Polar Lipids, USA) provided evidence of contacts between atoms of the N-terminal region of NTAc- α S and the membrane surface. The spectra showed selective paramagnetic broadening of ^{13}C - ^{13}C DARR resonances for both aliphatic-aliphatic and aliphatic-carbonyl cross-peaks, and suggested the topology of an amphipathic helix laying parallel on the membrane surface (Fig. 4). We then probed the degree of insertion of the N-terminal region of NTAc- α S into the hydrophobic region of the membrane by measuring PREs with paramagnetic lipids having spins at the positions of carbons 5, 10 and 16 of the lipid tail. These PRE experiments showed a gradual reduction of the paramagnetic broadening effect when changing the position of the spin from carbon 5 to carbon 16 of the lipid tail (Fig. 4), with the latter showing no evidence of PRE effect in the DARR spectrum.

These data indicate mild levels of insertion of the N-terminal region of NTAc- α S into the lipid bilayer, a result that is consistent with PRE experiments previously performed under the same experimental conditions by using non-acetylated α S^{44,58}.

Discussion

Although close links between PD and the aggregation of α S are widely recognised, the physiological role of this presynaptic protein remains largely unclear¹⁷. It has now become evident that a fundamental element for the biological activity of α S is the interaction with lipid membranes⁶⁶, which appears to be crucial in defining the balance between normal and aberrant forms of this protein. The membrane-binding affinity by α S is primarily influenced by the properties of the lipid bilayer, including curvature, charge, packing defects and surface hydrophobicity^{46,47,67-69}, but other factors such as calcium binding⁷⁰, phosphorylation⁴⁸⁻⁵⁰ and N-terminal acetylation^{51,52} have also been shown to modulate this interaction.

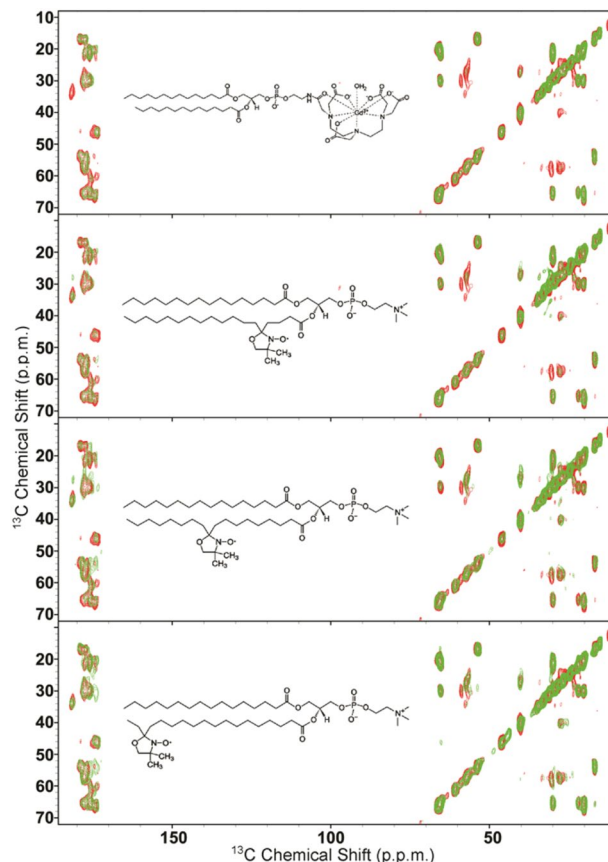


Figure 4. Membrane insertion properties of the N-terminal region of NTAc- α S using PREs. ssNMR PRE of membrane bound NTAc- α S were measured by doping to DOPE:DOPS:DOPC SUVs with 2% of lipid molecules having a paramagnetic centre in different positions ranging from the hydrophilic head group (1-palmitoyl-2-stearoyl-[5-doxyl]-sn-glycero-3-phosphocholine) to the position of carbons 5, 10 and 16 of the lipid tail (1-palmitoyl-2-stearoyl-[N-doxyl]-sn-glycero-3-phosphocholine, $N = 5, 10, 16$). The chemical structures of the paramagnetically labelled lipids are shown in the corresponding spectra. ^{13}C - ^{13}C -DARR spectra of these samples were measured at -19°C to favour the gel phase of the membrane⁴⁴, and using 1 ms and 50 ms for contact and mixing times, respectively. The experiments were performed at a ^1H Larmor frequency of 700 MHz using a 3.2 mm E^{Free} probe and a MAS rate of 10.0 kHz. Spectra in the presence and absence of the paramagnetic lipids are shown in green and red, respectively.

We have used here ssNMR spectroscopy to investigate the structure, dynamics and membrane-topology of NTAc- α S bound to synaptic-like vesicles. The acetylation of the N-terminal residue of α S is indeed prevalent in both healthy individuals and PD patients^{51–56}, and characterising its influence on the modes of membrane binding is crucial to understand biological behaviour of this protein. Previous solution NMR studies have probed this interaction by studying the properties of the unbound state of NTAc- α S in equilibrium with its membrane-bound form^{53,54}. The resulting spectra showed increased relaxation properties for the resonances of the N-terminal region of the protein indicating stronger membrane-binding for this region when the protein is acetylated. This result is consistent with the present chemical exchange saturation transfer (CEST) experiments that enabled to characterise the equilibrium between bound and unbound states at a residue-specific level (Fig. 5). CEST measurements also showed no significant decrease in the saturation of residues that immediately follow the N-terminal region, as observed in the non-acetylated case⁴⁴, indicating stronger membrane affinity for these residues in the case of NTAc- α S.

Despite these observations of higher membrane affinity in NTAc- α S, our ssNMR spectra indicate that this PTM does not alter the conformational properties of the membrane-bound state of the protein. In particular, cross polarisation and INEPT spectra, probing respectively rigid and highly dynamical regions of the protein (Figs. 2 and 3), indicated no substantial differences in the structure and dynamics of the membrane-bound states of NTAc- α S compared to non-acetylated α S⁴⁴. The analysis of the chemical shifts of the bound states of NTAc- α S and non-acetylated α S showed a similar content of α -helix in the N-terminal region (Fig. 2c), indicating a single binding mode for this protein segment in both protein constructs. Moreover ssNMR PRE experiments, provided evidence that the modes of membrane insertion of the N-terminal anchor of α S are not significantly altered by the N-terminal acetylation.

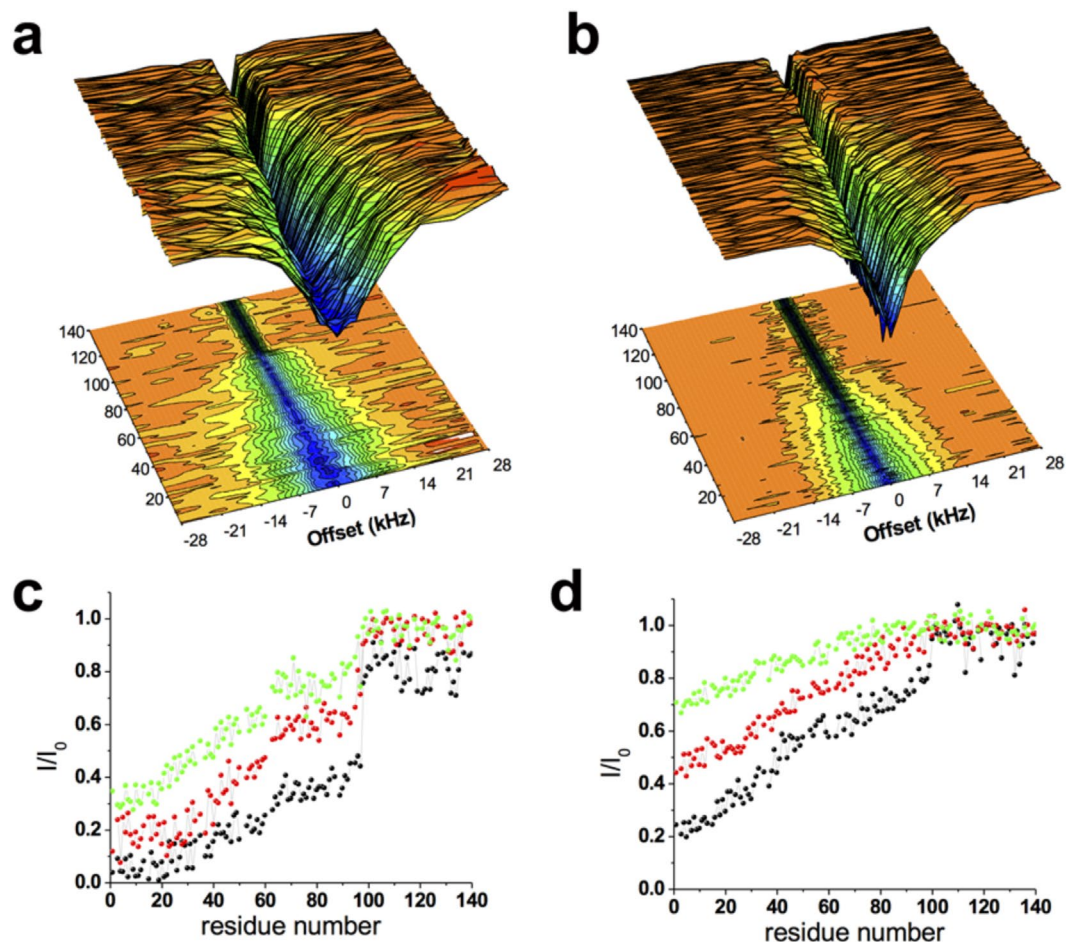


Figure 5. CEST experiments probing the binding equilibrium of NTAc- α S. CEST ^1H - ^{15}N HSQC spectra were recorded by applying a continuous wave saturation (170 Hz or 350 Hz) on the ^{15}N resonance with offsets ranging from -28 kHz to $+28$ kHz, and using a reference spectrum measured with an offset of 100 kHz. Measurements were carried out using a protein concentration of $300\ \mu\text{M}$ and 0.06% (0.6 mg/ml) of SUVs composed of DOPE:DOPS:DOPC lipids in a ratio of 5:3:2 (w/w). (**a,b**) CEST surfaces measured using bandwidths of 350 Hz and 170 Hz, respectively. (**c,d**) CEST saturation along the α S sequence measured using bandwidths of 350 Hz and 170 Hz, respectively. Black, red and green lines refer to the averaged CEST profiles measured using offsets at ± 1.5 kHz, ± 3 kHz and ± 5 kHz, respectively.

Taken together, these data indicate that the enhanced affinity of NTAc- α S for binding biological membranes is not the result of any specific alteration of its membrane-bound state, and suggest that it is likely promoted by changes in the properties of the unbound α S, particularly the increased α -helical character in the N-terminal region⁵³. The presence of transient α -helical conformations in the N-terminal region of the unbound NTAc- α S has the likely effect of relieving part of the entropic cost associated with the disorder-to-order transition required for the membrane binding. This intrinsic α -helical propensity may also favour the reversibility of the membrane interaction, which is essential to promote a rapid equilibrium between bound and unbound states, a key element for the ability of α S to facilitate the interaction between synaptic vesicles^{23–26}. This biological property has been associated with the putative function of α S of regulating distal pools of synaptic vesicles that play a key role for the SV homeostasis during neurotransmitter release^{20–22}.

In conclusion the topological and structural properties of the membrane-bound state of NTAc- α S that we have described here contribute to the definition of the mechanism by which the N-terminal acetylation regulates the mechanism of binding to synaptic membranes.

Methods

NTAc- α S purification. α S was expressed and purified as previously described⁴⁴. Briefly the protein was expressed in *E. coli* using plasmid pT7-7⁴⁴. In order to obtain N-terminal acetylation of α S we used coexpression with a plasmid carrying the components of the NatB complex (Addgene).

After transforming in BL21 (DE3)-gold cells (Agilent Technologies, Santa Clara, USA), uniformly ^{15}N and/or ^{13}C labeled α S variants were obtained by growing the bacteria in isotope-enriched M9 minimal media containing $1\ \text{g}\cdot\text{L}^{-1}$ of ^{15}N ammonium chloride, $2\ \text{g}\cdot\text{L}^{-1}$ of ^{13}C -glucose (Sigma-Aldrich, St Louis, USA) and 1 g of protonated

IsoGro ^{15}N - ^{13}C (Sigma, St. Louis, MO). The growth was obtained at 37°C under constant shaking at 250 rpm and supplemented with $100\ \mu\text{g}\cdot\text{ml}^{-1}$ ampicillin to an OD600 of 0.6. The expression was induced with 1 mM isopropyl β -D-1-thiogalactopyranoside (IPTG) at 37°C for 4 h, and the cells were harvested by centrifugation at 6200 g (Beckman Coulter, Brea, USA). The cell pellets were resuspended in lysis buffer (10 mM Tris-HCl pH 8, 1 mM EDTA and EDTA-free complete protease inhibitor cocktail tablets obtained from Roche, Basel, Switzerland) and lysed by sonication. The cell lysate was centrifuged at 22,000 g for 30 min to remove cell debris. In order to precipitate the heat-sensitive proteins, the supernatant was then heated for 20 min at 70°C and centrifuged at 22,000 g. Subsequently streptomycin sulfate was added to the supernatant to a final concentration of $10\ \text{mg}\cdot\text{ml}^{-1}$ to stimulate DNA precipitation. The mixture was stirred for 15 min at 4°C followed by centrifugation at 22,000 g. Then, ammonium sulfate was added to the supernatant to a concentration of $360\ \text{mg}\cdot\text{ml}^{-1}$ in order to precipitate the protein. The solution was stirred for 30 min at 4°C and centrifuged again at 22,000 g. The resulting pellet was resuspended in 25 mM Tris-HCl, pH 7.7 and dialyzed against the same buffer in order to remove salts. The dialyzed solutions were then loaded onto an anion exchange column (26/10 Q sepharose high performance, GE Healthcare, Little Chalfont, UK) and eluted with a 0–1 M NaCl step gradient, and then further purified by loading onto a size exclusion column (Hiload 26/60 Superdex 75 preparation grade, GE Healthcare, Little Chalfont, UK). All the fractions containing the monomeric protein were pooled together and concentrated by using Vivaspin filter devices (Sartorius Stedim Biotech, Gottingen, Germany). The purity of the aliquots after each step was analyzed by SDS-PAGE and the protein concentration was determined from the absorbance at 275 nm using an extinction coefficient of $5600\ \text{M}^{-1}\ \text{cm}^{-1}$. Mass spectrometry was used to assess that the level of N-terminal acetylation was complete.

Preparation of SUVs. Small unilamellar vesicles (SUVs) containing DOPE:DOPS:DOPC at a ratio of 5:3:2 (w/w) or POPG (Avanti Polar Lipids Inc., Alabaster, USA) were prepared from chloroform solutions of the lipids as described previously^{43,44}. Briefly, the lipid mixture was evaporated under a stream of nitrogen gas and then dried thoroughly under vacuum to yield a thin lipid film. The dried thin film was then re-hydrated by adding aqueous buffer (20 mM sodium phosphate, pH 6.0) at a concentration of $15\ \text{mg}\cdot\text{ml}^{-1}$ (1.5%) and subjected to vortex mixing. In all NMR experiments described in this paper SUVs were obtained by using several cycles of freeze-thawing and sonication until the mixture became clear^{43,44}. For ssNMR studies αS was added to the SUV mixtures up to a molar ratio of 1:65 protein:lipid. The mixtures were then pelleted at 303,747 g for 30 min at 4°C (Beckman Coulter Optima TLX Inc. Brea, USA) by using a TLA 100.3 rotor. Subsequently the SUV- αS samples were transferred into 3.2 mm Zirconia XC thin-walled MAS rotors for ssNMR experiments.

Magic angle spinning (MAS) measurements. MAS ssNMR measurements were used to directly probe the resonances of NTAc- αS in the vesicle-bound state, which are inaccessible to solution-state NMR. MAS experiments were carried out on a 700 MHz Bruker Spectrometer with a 3.2 mm E^{Free} probe. Dipolar assisted rotational resonance (DARR) experiments⁵⁹ were performed at a MAS rate of 10 kHz using a mixing time of 50 ms and a contact time of 1 ms. DARR spectra were acquired at -19°C to favour signal to noise by inducing a gel phase of the lipid membranes. Previous studies showed that the chemical shifts of αS bound to DOPE:DOPS:DOPC SUVs at -19°C and 4°C are indistinguishable, ruling out conformational changes of the protein as a result of the different phases of the lipids⁴⁴. Insensitive nuclei enhanced by polarization transfer (INEPT) spectra⁶² were measured at 4°C using a MAS rate of 10 kHz. Pulse widths were $2.5\ \mu\text{s}$ for ^1H and $5.5\ \mu\text{s}$ for ^{13}C , and ^1H TPPM decoupling was applied at $\omega_{\text{RF}}/(2\pi) = 71.4\text{--}100\ \text{kHz}$ ⁴⁴. ^1H detected ^1H - ^{15}N -HSQC of membrane bound NTAc- αS was measured as in Gopinath *et al.*⁶³. Assignments of the resonances of NTAc- αS in DARR and INEPT spectra were derived from our previous study of αS bound to SUVs or unbound αS ⁴⁴.

Chemical exchange saturation transfer (CEST) experiments. CEST measurements^{44,71–75} probed the equilibrium between membrane unbound and membrane bound states of αS *via* direct detection of saturation in the resonances of the unbound state. In studying αS -SUV interactions, CEST shows higher sensitivity than measurements based on the signal attenuation in HSQC spectra, which enables measurements at low lipid:protein ratios to minimise αS or lipid aggregation⁴⁴. Moreover, CEST signals are directly sensitive to the interaction between αS and the membrane surface and minimise the interference from additional factors that can contribute to the transverse relaxation rates of the protein resonances^{72–75}. Solution state NMR experiments were carried out at 10°C on a sample composed of αS ($300\ \mu\text{M}$) incubated with DOPE:DOPS:DOPC SUVs at a concentration of $0.6\ \text{mg}/\text{ml}$ and using a Bruker spectrometer operating at ^1H frequencies of 700 MHz equipped with triple resonance HCN cryo-probe. CEST experiments were based on ^1H - ^{15}N HSQC spectra by applying constant wave saturation in the ^{15}N channel. Assignment of the solution NMR resonances was obtained from our previous studies⁴⁴ and controlled with a series of 3D spectra by following a published protocol⁷⁶. Since we aimed at probing the exchange between monomeric αS (having sharp resonances) and αS bound to SUVs (having significantly broader resonances), a series of large offsets was employed ($-28, -21, -14, -9, -5, -3, -1.5, 0, 1.5, 3, 5, 9, 14, 21$ and $28\ \text{kHz}$), resulting in CEST profiles of symmetrical shapes^{44,72,73}. An additional spectrum, saturated at $-100\ \text{kHz}$, was recorded as a reference. The CEST experiments were measured using a data matrix consisting of $2048 (t_2, ^1\text{H}) \times 220 (t_1, ^{15}\text{N})$ complex points.

Received: 25 June 2019; Accepted: 2 December 2019;

Published online: 14 January 2020

References

- Jakes, R., Spillantini, M. G. & Goedert, M. Identification of two distinct synucleins from human brain. *FEBS Lett.* **345**, 27–32 (1994).
- Luk, K. C. *et al.* Pathological alpha-synuclein transmission initiates Parkinson-like neurodegeneration in nontransgenic mice. *Science* **338**, 949–53 (2012).

3. Uversky, V. N. & Eliezer, D. Biophysics of Parkinson's disease: structure and aggregation of alpha-synuclein. *Curr. Protein Pept. Sci.* **10**, 483–99 (2009).
4. Chiti, F. & Dobson, C. M. Protein Misfolding, Amyloid Formation, and Human Disease: A Summary of Progress Over the Last Decade. *Annu. Rev. Biochem.* **86**, 27–68 (2017).
5. Luth, E. S., Stavrovskaya, I. G., Bartels, T., Kristal, B. S. & Selkoe, D. J. Soluble, prefibrillar alpha-synuclein oligomers promote complex I-dependent, Ca²⁺-induced mitochondrial dysfunction. *J. Biol. Chem.* **289**, 21490–507 (2014).
6. Lashuel, H. A., Overk, C. R., Oueslati, A. & Masliah, E. The many faces of alpha-synuclein: from structure and toxicity to therapeutic target. *Nat. Rev. Neurosci.* **14**, 38–48 (2013).
7. Goedert, M., Spillantini, M. G., Del Tredici, K. & Braak, H. 100 years of Lewy pathology. *Nat. Rev. Neurol.* **9**, 13–24 (2013).
8. Bosco, D. A. *et al.* Elevated levels of oxidized cholesterol metabolites in Lewy body disease brains accelerate alpha-synuclein fibrillogenesis. *Nat. Chem. Biol.* **2**, 249–53 (2006).
9. Jucker, M. & Walker, L. C. Self-propagation of pathogenic protein aggregates in neurodegenerative diseases. *Nature* **501**, 45–51 (2013).
10. Polymeropoulos, M. H. *et al.* Mutation in the alpha-synuclein gene identified in families with Parkinson's disease. *Science* **276**, 2045–7 (1997).
11. Kruger, R. *et al.* Ala30Pro mutation in the gene encoding alpha-synuclein in Parkinson's disease. *Nat. Genet.* **18**, 106–8 (1998).
12. Singleton, A. B. *et al.* alpha-Synuclein locus triplication causes Parkinson's disease. *Science* **302**, 841 (2003).
13. Zarranz, J. J. *et al.* The new mutation, E46K, of alpha-synuclein causes Parkinson and Lewy body dementia. *Ann. Neurol.* **55**, 164–73 (2004).
14. Appel-Cresswell, S. *et al.* Alpha-synuclein p.H50Q, a novel pathogenic mutation for Parkinson's disease. *Mov. Disord.* **28**, 811–3 (2013).
15. Lesage, S. *et al.* & French Parkinson's Disease Genetics Study, G. G51D alpha-synuclein mutation causes a novel parkinsonian-pyramidal syndrome. *Ann. Neurol.* **73**, 459–71 (2013).
16. Ueda, K. *et al.* Molecular cloning of cDNA encoding an unrecognized component of amyloid in Alzheimer disease. *Proc. Natl Acad. Sci. USA* **90**, 11282–6 (1993).
17. Burre, J. The Synaptic Function of alpha-Synuclein. *J. Parkinsons Dis.* **5**, 699–713 (2015).
18. Vargas, K. J. *et al.* Synucleins regulate the kinetics of synaptic vesicle endocytosis. *J. Neurosci.* **34**, 9364–76 (2014).
19. Nemani, V. M. *et al.* Increased expression of alpha-synuclein reduces neurotransmitter release by inhibiting synaptic vesicle recluster after endocytosis. *Neuron* **65**, 66–79 (2010).
20. Cooper, A. A. *et al.* Alpha-synuclein blocks ER-Golgi traffic and Rab1 rescues neuron loss in Parkinson's models. *Science* **313**, 324–8 (2006).
21. Auluck, P. K., Caraveo, G. & Lindquist, S. alpha-Synuclein: membrane interactions and toxicity in Parkinson's disease. *Annu. Rev. Cell Dev. Biol.* **26**, 211–33 (2010).
22. Wislet-Gendebien, S. *et al.* Cytosolic proteins regulate alpha-synuclein dissociation from presynaptic membranes. *J. Biol. Chem.* **281**, 32148–55 (2006).
23. Fusco, G. *et al.* Structural basis of synaptic vesicle assembly promoted by alpha-synuclein. *Nat. Commun.* **7**, 12563 (2016).
24. Soper, J. H. *et al.* Alpha-synuclein-induced aggregation of cytoplasmic vesicles in *Saccharomyces cerevisiae*. *Mol. Biol. Cell* **19**, 1093–103 (2008).
25. Gitler, A. D. *et al.* The Parkinson's disease protein alpha-synuclein disrupts cellular Rab homeostasis. *Proc. Natl Acad. Sci. USA* **105**, 145–50 (2008).
26. Diao, J. *et al.* Native alpha-synuclein induces clustering of synaptic-vesicle mimics via binding to phospholipids and synaptobrevin-2/VAMP2. *Elife* **2**, e00592 (2013).
27. Burre, J., Sharma, M. & Sudhof, T. C. alpha-Synuclein assembles into higher-order multimers upon membrane binding to promote SNARE complex formation. *Proc. Natl Acad. Sci. USA* **111**, E4274–83 (2014).
28. Burre, J. *et al.* Alpha-synuclein promotes SNARE-complex assembly *in vivo* and *in vitro*. *Science* **329**, 1663–7 (2010).
29. Chandra, S., Gallardo, G., Fernandez-Chacon, R., Schluter, O. M. & Sudhof, T. C. Alpha-synuclein cooperates with CSPA in preventing neurodegeneration. *Cell* **123**, 383–96 (2005).
30. Pelkonen, A. & Yavich, L. Neuromuscular pathology in mice lacking alpha-synuclein. *Neurosci. Lett.* **487**, 350–3 (2011).
31. Menges, S. *et al.* Alpha-synuclein prevents the formation of spherical mitochondria and apoptosis under oxidative stress. *Sci. Rep.* **7**, 42942 (2017).
32. Maltsev, A. S., Chen, J., Levine, R. L. & Bax, A. Site-specific interaction between alpha-synuclein and membranes probed by NMR-observed methionine oxidation rates. *J. Am. Chem. Soc.* **135**, 2943–6 (2013).
33. Zigueanu, I. G., Yang, Y. J., Krois, A. S., Haque, E. & Pielak, G. J. Interaction of alpha-synuclein with vesicles that mimic mitochondrial membranes. *Biochim. Biophys. Acta* **1818**, 512–9 (2012).
34. Fusco, G., Sanz-Hernandez, M. & De Simone, A. Order and disorder in the physiological membrane binding of alpha-synuclein. *Curr. Opin. Struct. Biol.* **48**, 49–57 (2018).
35. Lee, H. J., Choi, C. & Lee, S. J. Membrane-bound alpha-synuclein has a high aggregation propensity and the ability to seed the aggregation of the cytosolic form. *J. Biol. Chem.* **277**, 671–8 (2002).
36. Galvagnion, C. *et al.* Lipid vesicles trigger alpha-synuclein aggregation by stimulating primary nucleation. *Nat. Chem. Biol.* **11**, 229–34 (2015).
37. Comellas, G., Lemkau, L. R., Zhou, D. H., George, J. M. & Rienstra, C. M. Structural intermediates during alpha-synuclein fibrillogenesis on phospholipid vesicles. *J. Am. Chem. Soc.* **134**, 5090–9 (2012).
38. Necula, M., Chirita, C. N. & Kuret, J. Rapid anionic micelle-mediated alpha-synuclein fibrillization *in vitro*. *J. Biol. Chem.* **278**, 46674–80 (2003).
39. Zhu, M. & Fink, A. L. Lipid binding inhibits alpha-synuclein fibril formation. *J. Biol. Chem.* **278**, 16873–7 (2003).
40. Perrin, R. J., Woods, W. S., Clayton, D. F. & George, J. M. Exposure to long chain polyunsaturated fatty acids triggers rapid multimerization of synucleins. *J. Biol. Chem.* **276**, 41958–62 (2001).
41. Sharon, R. *et al.* The formation of highly soluble oligomers of alpha-synuclein is regulated by fatty acids and enhanced in Parkinson's disease. *Neuron* **37**, 583–95 (2003).
42. Fusco, G. *et al.* Structural basis of membrane disruption and cellular toxicity by alpha-synuclein oligomers. *Science* **358**, 1440–1443 (2017).
43. Bodner, C. R., Dobson, C. M. & Bax, A. Multiple tight phospholipid-binding modes of alpha-synuclein revealed by solution NMR spectroscopy. *J. Mol. Biol.* **390**, 775–90 (2009).
44. Fusco, G. *et al.* Direct observation of the three regions in alpha-synuclein that determine its membrane-bound behaviour. *Nat. Commun.* **5**, 3827 (2014).
45. Eliezer, D., Kutluay, E., Bussell, R. Jr. & Browne, G. Conformational properties of alpha-synuclein in its free and lipid-associated states. *J. Mol. Biol.* **307**, 1061–73 (2001).
46. Ulmer, T. S., Bax, A., Cole, N. B. & Nussbaum, R. L. Structure and dynamics of micelle-bound human alpha-synuclein. *J. Biol. Chem.* **280**, 9595–603 (2005).
47. Jao, C. C., Hegde, B. G., Chen, J., Haworth, I. S. & Langen, R. Structure of membrane-bound alpha-synuclein from site-directed spin labeling and computational refinement. *Proc. Natl Acad. Sci. USA* **105**, 19666–71 (2008).

48. Samuel, F. *et al.* Effects of Serine 129 Phosphorylation on alpha-Synuclein Aggregation, Membrane Association, and Internalization. *J. Biol. Chem.* **291**, 4374–85 (2016).
49. Dikiy, I. *et al.* Semisynthetic and *in Vitro* Phosphorylation of Alpha-Synuclein at Y39 Promotes Functional Partly Helical Membrane-Bound States Resembling Those Induced by PD Mutations. *ACS Chem. Biol.* **11**, 2428–37 (2016).
50. Kang, L. *et al.* N-terminal acetylation of alpha-synuclein induces increased transient helical propensity and decreased aggregation rates in the intrinsically disordered monomer. *Protein Sci.* **21**, 911–7 (2012).
51. Fauvet, B. *et al.* Characterization of semisynthetic and naturally N-alpha-acetylated alpha-synuclein *in vitro* and in intact cells: implications for aggregation and cellular properties of alpha-synuclein. *J. Biol. Chem.* **287**, 28243–62 (2012).
52. Burre, J. *et al.* Properties of native brain alpha-synuclein. *Nature* **498**, E4–6; discussion E6–7 (2013).
53. Maltsev, A. S., Ying, J. & Bax, A. Impact of N-terminal acetylation of alpha-synuclein on its random coil and lipid binding properties. *Biochemistry* **51**, 5004–13 (2012).
54. Dikiy, I. & Eliezer, D. N-terminal acetylation stabilizes N-terminal helicity in lipid- and micelle-bound alpha-synuclein and increases its affinity for physiological membranes. *J. Biol. Chem.* **289**, 3652–65 (2014).
55. Miotto, M. C. *et al.* Copper binding to the N-terminally acetylated, naturally occurring form of alpha-synuclein induces local helical folding. *J. Am. Chem. Soc.* **137**, 6444–7 (2015).
56. Moriarty, G. M., Minetti, C. A., Remeta, D. P. & Baum, J. A revised picture of the Cu(II)-alpha-synuclein complex: the role of N-terminal acetylation. *Biochemistry* **53**, 2815–7 (2014).
57. Kang, L., Janowska, M. K., Moriarty, G. M. & Baum, J. Mechanistic insight into the relationship between N-terminal acetylation of alpha-synuclein and fibril formation rates by NMR and fluorescence. *PLoS One* **8**, e75018 (2013).
58. Fusco, G. *et al.* Structural Ensembles of Membrane-bound alpha-Synuclein Reveal the Molecular Determinants of Synaptic Vesicle Affinity. *Sci. Rep.* **6**, 27125 (2016).
59. Takegoshi, K. & Terao, T. ¹³C-1H dipolar recoupling under very fast magic-angle spinning using virtual pulses. *Solid. State Nucl. Magn. Reson.* **13**, 203–12 (1999).
60. Nagle, J. F. & Tristram-Nagle, S. Structure of lipid bilayers. *Biochim. Biophys. Acta* **1469**, 159–95 (2000).
61. Lokappa, S. B. & Ulmer, T. S. Alpha-synuclein populates both elongated and broken helix states on small unilamellar vesicles. *J. Biol. Chem.* **286**, 21450–7 (2011).
62. Morris, G. A. & Freeman, R. Enhancement of Nuclear Magnetic-Resonance Signals by Polarization Transfer. *J. Am. Chem. Soc.* **101**, 760–762 (1979).
63. Gopinath, T., Nelson, S. E. D., Soller, K. J. & Veglia, G. Probing the Conformationally Excited States of Membrane Proteins via (1) H-Detected MAS Solid-State NMR Spectroscopy. *J. Phys. Chem. B* **121**, 4456–4465 (2017).
64. Gustavsson, M. *et al.* Allosteric regulation of SERCA by phosphorylation-mediated conformational shift of phospholamban. *Proc. Natl Acad. Sci. USA* **110**, 17338–43 (2013).
65. Vicari, C. *et al.* Artificial heme-proteins: determination of axial ligand orientations through paramagnetic NMR shifts. *Chem. Commun. (Camb.)* **50**, 3852–5 (2014).
66. Snead, D. & Eliezer, D. Alpha-synuclein function and dysfunction on cellular membranes. *Exp. Neurobiol.* **23**, 292–313 (2014).
67. Rao, J. N., Jao, C. C., Hegde, B. G., Langen, R. & Ulmer, T. S. A combinatorial NMR and EPR approach for evaluating the structural ensemble of partially folded proteins. *J. Am. Chem. Soc.* **132**, 8657–68 (2010).
68. Ulmer, T. S. & Bax, A. Comparison of structure and dynamics of micelle-bound human alpha-synuclein and Parkinson disease variants. *J. Biol. Chem.* **280**, 43179–87 (2005).
69. Ouberaï, M. M. *et al.* alpha-Synuclein senses lipid packing defects and induces lateral expansion of lipids leading to membrane remodeling. *J. Biol. Chem.* **288**, 20883–95 (2013).
70. Lautenschlager, J. *et al.* C-terminal calcium binding of alpha-synuclein modulates synaptic vesicle interaction. *Nat. Commun.* **9**, 712 (2018).
71. Romano, M. *et al.* Structural Basis for Natural Product Selection and Export by Bacterial ABC Transporters. *ACS Chem. Biol.* **13**, 1598–1609 (2018).
72. Huang, H., Milojevic, J. & Melacini, G. Analysis and optimization of saturation transfer difference NMR experiments designed to map early self-association events in amyloidogenic peptides. *J. Phys. Chem. B* **112**, 5795–802 (2008).
73. Fawzi, N. L., Ying, J., Ghirlando, R., Torchia, D. A. & Clore, G. M. Atomic-resolution dynamics on the surface of amyloid-beta protofibrils probed by solution NMR. *Nature* **480**, 268–72 (2011).
74. Vallurupalli, P., Bouvignies, G. & Kay, L. E. Studying “invisible” excited protein states in slow exchange with a major state conformation. *J. Am. Chem. Soc.* **134**, 8148–61 (2012).
75. Milojevic, J., Esposito, V., Das, R. & Melacini, G. Understanding the molecular basis for the inhibition of the Alzheimer’s Aβ-peptide oligomerization by human serum albumin using saturation transfer difference and off-resonance relaxation NMR spectroscopy. *J. Am. Chem. Soc.* **129**, 4282–90 (2007).
76. Fusco, G. *et al.* (1)H, (1)(3)C and (1)(5)N resonance assignments of human muscle acylphosphatase. *Biomol. NMR Assign.* **6**, 27–9 (2012).
77. Camilloni, C., De Simone, A., Vranken, W. F. & Vendruscolo, M. Determination of Secondary Structure Populations in Disordered States of Proteins Using Nuclear Magnetic Resonance Chemical Shifts. *Biochemistry* **51**, 2224–2231 (2012).

Acknowledgements

This research is supported by Parkinson’s UK (G-1508, A.D., M.V., C.M.D. and G.F.), the UK Medical Research Council (MR/N000676/1, A.D., M.V. and C.M.D.), the European Research Council (ERC) Consolidator Grant (CoG) ‘BioDisOrder’ (819644, A.D.), The Centre for Misfolding Diseases of the University of Cambridge (C.M.D. and M.V.) and the St John’s College Fellowship (G.F.).

Author contributions

G.F., A.D. and C.M.D. conceived the experiments. M.R., A.D. and G.F. conducted the experiments. All authors analysed and discussed the results. A.D., M.V. and G.F. wrote the manuscript with input from all authors.

Competing interests

The authors declare no competing interests.

Additional information

Correspondence and requests for materials should be addressed to G.F.

Reprints and permissions information is available at www.nature.com/reprints.

Publisher’s note Springer Nature remains neutral with regard to jurisdictional claims in published maps and institutional affiliations.



Open Access This article is licensed under a Creative Commons Attribution 4.0 International License, which permits use, sharing, adaptation, distribution and reproduction in any medium or format, as long as you give appropriate credit to the original author(s) and the source, provide a link to the Creative Commons license, and indicate if changes were made. The images or other third party material in this article are included in the article's Creative Commons license, unless indicated otherwise in a credit line to the material. If material is not included in the article's Creative Commons license and your intended use is not permitted by statutory regulation or exceeds the permitted use, you will need to obtain permission directly from the copyright holder. To view a copy of this license, visit <http://creativecommons.org/licenses/by/4.0/>.

© The Author(s) 2020